cluding ions trapped in C_{60} (*18*) and ship-in-a-bottle synthesis of ions trapped in zeolites (*19*), the distinctive materials produced with our method are monolayer, room-temperature matrices that hold molecularly dispersed polyatomic cations. The implications for spectroscopy are apparent. The placement of isolated ions a few angstroms from a metal should give rise to interesting spectroscopic effects associated with the mixing of the discrete molecular orbitals of the matrix-isolated ions and the diffuse bands of the metal. The potential for preparing surfaces and interfaces with unusual electronic and magnetic properties is also evident. The extraordinary selectivity offered by the availability of a wide variety of projectile ions should allow the production of long-lived metastable structures of various types at self-assembled monolayer surfaces.

REFERENCES AND NOTES

1. A. Aviram, *Molecular Electronics: Science and Technology* (American Institute of Physics, New York, 1992); E. Kim, G. M. Whitesides, L. K. Lee, S. P. Smith, M. Prentiss, *Adv. Mater.* **8**, 139 (1996); K. K. Berggren *et al.*, *Science* **269**, 1255 (1995); D. Li *et al.*, *J. Am. Chem. Soc.* **112**, 7389 (1990); A. J. Bard *et al.*, *J. Phys. Chem.* **97**, 7147 (1993).
2. J. Shi *et al.*, *Nature* **377**, 707 (1995).
3. J. W. Rabalais and S. R. Kasi, *Science* **239**, 623 (1988).
4. H. Kang, S. R. Kasi, J. W. Rabalais, *J. Chem. Phys.* **88**, 5882 (1988).
5. D. Strongin and J. Mowlem, *Chem. Phys. Lett.* **187**, 281 (1991).
6. R. G. Cooks, T. Ast, T. Pradeep, V. H. Wysocki, *Acc. Chem. Res.* **27**, 316 (1994); T. Pradeep *et al.*, *J. Am. Soc. Mass Spectrom.* **6**, 187 (1995).
7. M. D. Porter, T. B. Bright, D. L. Allara, C. E. D. Chidsey, *J. Am. Chem. Soc.* **109**, 3559 (1987); F. Sun *et al.*, *ibid.* **118**, 1856 (1996).
8. For early attempts to perform this experiment, see V. Franchetti, B. H. Solka, W. E. Baitinger, J. W. Amy, R. G. Cooks, *Int. J. Mass Spectrom. Ion Phys.* **23**, 29 (1977).
9. R. G. Cooks, T. Ast, M. A. Mabud, *Int. J. Mass Spectrom. Ion Processes* **100**, 209 (1990); J. L. Jones, A. R. Dongre, A. Somogyi, V. H. Wysocki, *J. Am. Chem. Soc.* **116**, 8368 (1994); Q. Wu and L. Hanley, *ibid.* **115**, 1191 (1993); W. R. Koppers *et al.*, *Phys. Rev. B* **53**, 11207 (1996); M. J. Hayward *et al.*, *J. Am. Chem. Soc.* **118**, 8375 (1996).
10. The image in Fig. 1 was produced with the program CAChe, version 3.7 (CAChe Scientific, Beaverton, OR).
11. F-SAM chain spacings were set according to G. Liu *et al.*, *J. Chem. Phys.* **101**, 4301 (1994).
12. F-SAM surfaces were prepared by soaking the substrate in a 1 mM solution of $CF_3(CF_2)_7(CH_2)_2SH$ in ethanol for at least a few days. The surfaces were then rinsed and sonicated in ethanol several times before modification by the low-energy ion beams. The substrate consists of a glass layer, 1.6 mm thick, covered with 50 Å of Ti and 1000 Å of polycrystalline gold.
13. Beam sizes were estimated using a highly focused 15-keV beam of Ga^+ after modification of two F-SAM surfaces at 10 eV (area 50 mm^2) and 60 eV (area 3 mm^2).
14. The number of sputtered ions was estimated by converting the total analog-to-digital converter counts in the sputtered ion decay curve of the deposited species into an ion current and estimating corrections for the gain, transmission, and spot sizes of the experiment.
15. The high-resolution TOF-SIMS analysis was performed with a TFS series instrument (Charles Evans & Associates, Redwood City, CA) with 15-keV Ga^+ ion sputtering. The TOF-SIMS data were taken about 36 hours after the surface sample was modified with $C_3H_{10}Si_2O^{35}Cl^+$ (*m/z* 153) and $C_3H_{10}Si_2O^{37}Cl^+$ (*m/z* 155) from projectile ions $C_5H_{14}Si_2O^{35}Cl^+$ (*m/z* 181) and $C_5H_{14}Si_2O^{37}Cl^+$ (*m/z* 183), respectively. The ions $C_3H_{10}Si_2O^{35}Cl^+$ (*m/z* 153) and $C_3H_{10}Si_2O^{37}Cl^+$ (*m/z* 155) had about equal intensities as determined by in situ 60-eV $^{132}Xe^{\cdot+}$ sputtering analysis before the sample was sent to 3M Center (St. Paul, MN) for TOF-SIMS analysis.
16. The cross section for sputtered ion yields is maximized when the recombination energy is in resonance with the ionization energy of the neutral molecule [see J. B. Hasted, *Physics of Atomic Collisions* (American Elsevier, New York, ed. 2, 1972), p. 612]. Neutralization and deposition of the resulting radicals into the surface is not precluded; this is likely to be one of the ion loss processes leading to low yields.
17. These experiments were performed with a Finnigan TSQ 700 triple-quadrupole mass spectrometer with the ion source filament turned off. The sample was mounted on a specially constructed direct insertion probe that heated the surface from room temperature to 400°C in 40 s. Well-defined peaks from desorbed ions were observed in plots of ion abundance versus time. The trapped ions that are thermally released might not be as tightly held as those desorbed by ion impact.
18. R. Tellgmann, N. Krawez, S.-H. Lin, I. V. Hertel, E. E. B. Campbell, *Nature* **382**, 407 (1996).
19. T. Tao and G. Maciel, *J. Am. Chem. Soc.* **117**, 12889 (1995).

20. Supported by NSF grant CHE-9223791. We thank B. Feng for assistance in the F-SAM surface preparation, D. Lantrip for the CAChe simulations, G. Chen for the triple-quadrupole data, Y. H. Yim for the trifluoromethylbenzoyl data, and T. Bein, W. N. Delgass, B. S. Freiser, H. W. Rohrs, and V. H. Wysocki for helpful comments.

15 October 1996; accepted 9 January 1997

Gliding Mechanism in the Late Permian Reptile *Coelurosauravus*

Eberhard Frey, Hans-Dieter Sues,* Wolfgang Munk

A complete skeleton of the oldest known flying reptile, *Coelurosauravus jaekeli,* from the Upper Permian of Germany, and reexamination of other specimens demonstrate that this animal had a gliding apparatus unlike that of any other tetrapod. The lateral gliding membrane was supported by radially disposed, greatly elongated bony rods of dermal origin in the thoracolumbar region, rather than by internal skeletal elements such as ribs and limb bones. The rods are independent of the ribcage and arranged in distinct bundles to form a cambered wing.

Extant and fossil terrestrial vertebrates have developed a diversity of gliding mechanisms (*1, 2*): (i) flattening of the body by drawing in the ventral surface of the body (the flying snake, *Chrysopelea*); (ii) spreading of webbed feet or membranous flaps along the hind edges of the limbs, in some instances accompanied by flattening of the body (some flying frogs such as *Hyla miliaria* and *Rhacophorus rheinwardtii*); (iii) expansion of a lateral skin fold between the fore- and hindlimbs [flying phalangers (Marsupialia), flying lemurs (Dermoptera), and flying squirrels]; (iv) expansion of a lateral membrane supported by elongated, flexible thoracolumbar ribs [as in the gliding lizard *Draco* (*3*)]; and (v), as (iv), but with elongated, rigid ribs, which form hinge-joints with the considerably enlarged transverse processes of the dorsal vertebrae [Late Triassic Kuehneosauridae (*4, 5*)]. Although many birds, especially large forms, are skilled gliders, bats rarely glide, perhaps because they cannot control gliding and vary wing area as much as birds can (*2*). Here we describe a new skeleton of the oldest known flying tetrapod, *Coelurosauravus* (*6, 7*), and show that it had a different gliding mechanism from those examples mentioned above.

The Late Permian *Coelurosauravus* is a small diapsid reptile most closely related to the Neodiapsida, the clade including all archosaurian and lepidosaurian reptiles (*8*). The most diagnostic features of *Coelurosauravus* are the chameleon-like frill at the back of the skull roof, formed primarily by the squamosals, and the presence of numerous long, rodlike bones that supported a lateral gliding membrane (*8, 9*). These rods were originally misinterpreted as the fin rays of a coelacanth fish superimposed on a small reptilian skeleton and were, for the most part, removed during preparation of the holotype of *Coelurosauravus jaekeli* (*10*). When correctly recognized as genuine parts of the skeleton in other specimens, they were first interpreted as greatly elongated ribs (*11*) and later as the long distal segments of bipartite ribs (*8*). However, the supposed proximal rib elements (*8*) are short and strongly curved, much like the dorsal ribs in most other small reptiles. This feature is especially evident in an excellent-

---

E. Frey and W. Munk, Staatliches Museum für Naturkunde Karlsruhe, Erbprinzenstrasse 13, D-76133 Karlsruhe, Germany.
H.-D. Sues, Department of Palaeobiology, Royal Ontario Museum, 100 Queen's Park, Toronto, ON M5S 2C6, and Department of Zoology, University of Toronto, Toronto, ON M5S 3G5, Canada. E-mail: hdsues@rom.on.ca

* To whom correspondence should be addressed.

Fig. 1. *Coelurosauravus jaekeli*, SMNK 2882 PAL, nearly complete skeleton. Note the numerous long rods for support of a lateral gliding membrane and the very long tail. Image width, ~23 cm.

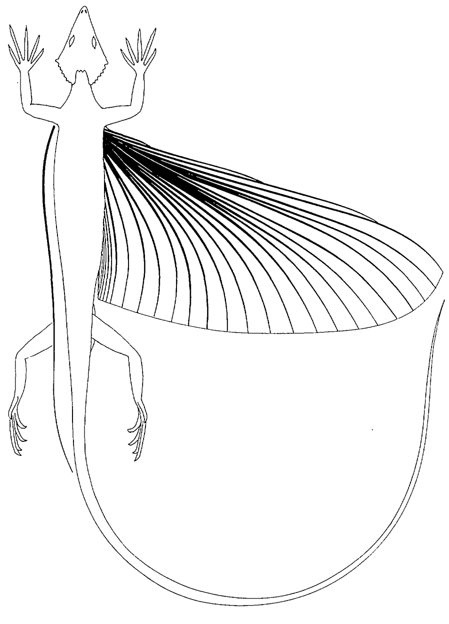

Fig. 2. Outline reconstruction of *C. jaekeli* in dorsal view, with the left wing folded against the body and the right wing fully spread. Body proportions are based on SMNK 2882 PAL (with a reconstructed snout-vent length of 18 cm). Details of individual bundles of rods were reconstructed on the basis of that fossil and the Eppleton specimen. The distal portions of the larger rods are shown as curved backward as a result of tension produced by the intervening gliding membrane when the wing is spread. The exact number and disposition of the small, delicate rods near the posterior margin of the wing is uncertain.

ly preserved partial skeleton from the Marl Slate of Eppleton Quarry (northeast England) (*8, 9*). The curvature of these ribs would rule out distal articulation with the rodlike elements. Furthermore, the inferred one-to-one correspondence between proximal ribs and distal rods would result in an improbably long thoracolumbar region comprising 24 to 28 vertebrae (*8, 12*).

An almost complete skeleton of *C. jaekeli* (Fig. 1) has only 13 thoracolumbar vertebrae but at least 22 rods on each side. This fossil demonstrates that, contrary to previous reports (*8*), the Eppleton specimen with 12 dorsal vertebrae, and a partial skeleton from the Kupferschiefer of Bodental, Hesse, with 13 (*8, 12, 13*), both preserve most or all of the thoracolumbar region. The anterior seven rods in the new specimen form a distinct bundle. A second bundle consists of five, a third of four, a fourth of three, and a fifth of two rods. The posterior six or seven rods appear to be single rods. Corresponding bundles with identical numbers of rods are preserved in the Eppleton skeleton and in a specimen from the Kupferschiefer of Bauhaus, Hesse (*13*). The arrangement of the bundles in the fossils indicates that the wing segments could be folded over each other when the wing was brought back against the body. In life, the configuration of bundles would have produced an anteroposteriorly curved (cambered) gliding membrane, which was ideally suited to its function as an airfoil.

Expansion of a lateral gliding membrane supported by rods is only possible when the rods are arranged in a more or less radial fashion. The Eppleton specimen shows that the anterior rods had a radial disposition, and, along with the Ellrich skeleton, demonstrates that the first bundle includes the longest rods supporting the wing. The rods in the more posterior bundles become progressively shorter (Fig. 2). If the right wing of the Eppleton fossil represents a relaxed, almost unfolded position of this structure, the leading edge of the wing of *Coelurosauravus* was oriented at an angle of about 45° to the long axis of the body. The trailing edge is marked by the distal ends of the more posterior rods. The long, flexible tail of *Coelurosauravus* (Fig. 2) may have aided in stabilization and steering during flight, much as in extant *Draco* and gliding mammals (*9*).

We interpret the elongated rods in *Coelurosauravus* as neomorphic dermal ossifications that formed the internal support of a lateral gliding membrane. Our scanning electron microscopy (SEM) investigation of samples removed from the new skeleton reveals that the rods are hollow and have thin walls with external sculpturing composed of fine longitudinal grooves and ridges. The gliding mechanism did not involve the thoracolumbar ribcage (*12*). The forelimbs were also not integrated into the membrane but may have aided in steering during gliding flight.

Coelurosauravus predates the next oldest known reptilian gliders, the Late Triassic Kuehneosauridae (*4, 5*), by at least 20 million years. Unlike in other tetrapods, the lateral gliding membrane in *Coelurosauravus* was entirely supported by independent, rodlike dermal mineralizations, rather than by internal skeletal elements.

Gliding could be used to facilitate escape from predators and for energy-efficient foraging in terrain with varied topography (*14*). Present-day gekkonid lizards provide an excellent structural model for the development of a lateral gliding membrane. The parachuting membrane of the flying gecko *Ptychozoon* developed from a lateral skin fold on the body (*14*). As in *Coelurosauravus*, it does not involve the limbs or ribcage.

REFERENCES AND NOTES

1. J. M. V. Rayner, in *Vertebrate Locomotion*, M. H. Day, Ed. (Academic Press, London, 1981), pp. 137–172.
2. U. M. Norberg, *Vertebrate Flight* (Springer-Verlag, Berlin, 1990).
3. E. H. Colbert, *Am. Mus. Novit.* **2283**, 1 (1967).
4. P. L. Robinson, *Proc. Geol. Soc. London* **1601**, 137 (1962).
5. E. H. Colbert, *Bull. Am. Mus. Nat. Hist.* **143**, 85 (1970).
6. *Coelurosauravus jaekeli* (Weigelt, 1930) is now known from several skeletons from the Kupferschiefer of Germany [originally described as *Palaeochamaeleo* or *Weigeltisaurus* (*8, 10*)] and the correlative Marl Slate of England (*8, 9*). The very closely related, possibly synonymous, *C. elivensis* [including *Daedalosaurus madagascariensis* (*8, 11*)] is represented by specimens from the Lower Sakamena Formation of Madagascar. The stratigraphic age of the Kupferschiefer and Lower Sakamena Formation is now considered latest Permian (Tatarian) [H.-D.

Sues and W. Munk, *Palaeontol. Z.* **70**, 213 (1996)].
7. The new skeleton was collected from the Kupferschiefer of Ellrich, Thuringia (Germany), and is now housed in the Staatliches Museum für Naturkunde Karlsruhe (SMNK 2882 PAL). It is almost complete and mostly articulated. The vertebral column is coiled, presumably due to postmortem desiccation.
8. S. E. Evans, *Zool. J. Linn. Soc.* **76**, 97 (1982); S. E. Evans and H. Haubold, *ibid.* **90**, 275 (1987).
9. T. H. Pettigrew, *Nature* **281**, 297 (1979).
10. J. Weigelt, *Nova Acta Leopold.* **6**, 625 (1930).
11. R. L. Carroll, *Palaeont. Afr.* **21**, 143 (1978).
12. G. Schaumberg, *Palaeontol. Z.* **60**, 319 (1986). Schaumberg first questioned the interpretation of the rods as rib elements proposed by Evans (*8*), but, with the fossils of *C. jaekeli* known at that time, he could not establish the arrangement and true nature of the rods.
13. The Bauhaus specimen is housed in the private collection of W. Simon, Cornberg (Germany), and the Bodental skeleton in the collection of P. Bürger, Bad Hersfeld (Germany). High-fidelity casts of these fossils have been deposited in the collections of the Staatliches Museum für Naturkunde Karlsruhe and the Royal Ontario Museum.
14. A. P. Russell, *Zool. J. Linn. Soc.* **65**, 233 (1979).
15. We thank the Royal Ontario Museum Foundation and Staatliches Museum für Naturkunde Karlsruhe for financial support, the authorities of the Sunderland Museum for permission to examine the Eppleton specimen, and P. Bürger and W. Simon for access to material in their private collections. B. Herkner, C. McGowan, and an anonymous reviewer provided constructive comments on a draft of the manuscript. U. Greiner and B. Boyle assisted with photography.

5 December 1996; accepted 16 January 1997

Strontianite in Coral Skeletal Aragonite

Robert B. Greegor, Nicholas E. Pingitore Jr.,* Farrel W. Lytle

An x-ray spectroscopic study of scleractinian coral skeletons indicated that, although some strontium substitutes for calcium in the aragonite structure, at concentrations of about 7500 parts per million, as much as 40 percent of the strontium resides in strontianite ($SrCO_3$). A doublet peak in the Fourier transform of the extended x-ray absorption fine structure of the coral corresponded to six metal and 13 oxygen neighbors surrounding strontium at about 4.05 angstroms in strontium-substituted aragonite and at about 4.21 angstroms in strontianite. Thus, the mechanism of the temperature-sensitive partitioning of strontium between seawater and coral skeleton used for paleothermometry is unexpectedly complex.

Strontium/calcium ratios in scleractinian corals have been used to reconstruct past sea surface temperatures (SSTs) on the basis of the observed temperature dependence of Sr partitioning between seawater and coral skeleton (*1*). However, in some cases SSTs derived from Sr/Ca ratios differ from those derived by other techniques (for example, oxygen isotopes), and the origins of these differences are not clear (*2*). Because $SrCO_3$ is isomorphous (*3*) and shows at least partial solid solution with aragonite (*4*), it generally has been thought (*4*, *5*) that Sr substitutes for Ca in biogenic and inorganic marine aragonites, although there is recent evidence to the contrary (*6*).

To characterize the site of Sr in aragonite scleractinian corals, we used x-ray absorption near-edge structure (XANES) and extended x-ray absorption fine structure (EXAFS) spectroscopy. In these experiments, an intense, monochromatic beam of x-rays, usually from a synchrotron source, is tuned gradually across the energy of a specific absorption edge of the element of interest, in this case Sr. Excitation and backscattering of Sr K-edge electrons provide information about the local environment (out to several nearest-neighbor shells) of the Sr atoms, at Sr concentrations as low as 1000 parts per million (ppm).

We analyzed four *Montastrea annularis* (MA) corals (one of Holocene age, one collected live, one collected live and then bleached, and one collected dead; all had ~7000 ppm of Sr), three *Acropora palmata* (AP) corals (one of Pleistocene age and two collected live; all had ~7500 ppm of Sr), and an aragonitic pelecypod bivalve (with ~1500 ppm of Sr) (*7*). We used calcite, inorganic aragonite, $SrCO_3$, SrO, and SrO_2 as standards for structural comparison and extraction of EXAFS phase shifts and scattering amplitudes. Measurements were conducted at the Stanford Synchrotron Radiation Laboratory (SSRL) using XAS techniques (*8*).

The aragonite and calcite XANES (Fig. 1) were taken at the Ca K-edge (4038.5 eV), whereas the other spectra were taken at the Sr K-edge (16104.6 eV). In calcite, Ca and Sr are distinguished from the other structural sites by a distinctive doublet at the top of the absorption rise for calcite and Sr in calcite. Fourier transforms of the K^3-weighted EXAFS data (from ~3.5 to 12 Å^{-1}) at the K-edges corresponding to the XANES, along with the appropriate phase shift (Ca-O or Sr-O), yielded peaks close to the expected crystallographic distances (Table 1). The measured metal-metal distances are also close to the reference distances established by x-ray diffraction (XRD) (*9*).

The Sr K-edge XANES of the different coral species and ages appear identical at the resolution presented in Fig. 2. The absence of the doublet at the top of absorption rise indicates that Sr is not in the calcite form of $CaCO_3$. The XANES features resemble Sr in $SrCO_3$, SrO_2, and SrO, and to a lesser extent, Ca in aragonite (Fig. 1).

Table 1. Summary of Fourier transforms, XRD, and least-squares fits to EXAFS data. N_f, coordination number (±20%) from least-squares fit; R_f, bond length (±0.05 Å) from least-squares fit; $\Delta\sigma^2$, mean-squared relative displacement (with respect to SrO standard) from least-squares fit; E_0, inner potential (treated as arbitrary parameter) from least-squares fit; SD, standard deviation of least-squares fit to data; R_t, bond length from peak of Fourier transform; XRD, x-ray diffraction data for coordination number and bond length; Sr, strontium in aragonite sample; MA, *M. annularis* coral; AP, *A. palmata* coral; PEL, pelecypod bivalve; H, Holocene age; P, Pleistocene age; l, collected live; d, collected dead; b, bleached. Calcite (rhombohedral) and aragonite (orthorhombic) are polymorphs of $CaCO_3$; $SrCO_3$ is isomorphous with aragonite.

Sample	N_f	R_f (Å)	$\Delta\sigma^2$ (Å^2)	E_0 (eV)	SD	R_t (Å)	XRD (Å)
Calcite						2.36	VI-2.36
Aragonite						2.53	IX-2.53
SrO						2.58	VI-2.58
SrO_2	10.6	2.57	0.0030	1.17	0.187	2.57	X-2.61
Strontianite	9.0	2.59	0.0006	0.44	0.189	2.64	IX-2.64
Sr (MA l)	8.8	2.55	−0.0004	0.00	0.225	2.57	
Sr (MA l, b)	8.6	2.56	−0.0006	0.17	0.274	2.57	
Sr (MA d)	9.3	2.56	−0.0002	0.56	0.202	2.57	
Sr (MA H)	8.8	2.56	−0.0008	1.01	0.273	2.60	
Sr (AP l-14)	8.8	2.56	−0.0007	0.29	0.294	2.57	
Sr (AP l-15)	8.9	2.55	−0.0003	0.30	0.286	2.57	
Sr (AP P)	8.9	2.55	−0.0004	−0.31	0.284	2.60	
Sr (PEL)	9.6	2.55	0.0007	0.14	0.253	2.52	

R. B. Greegor, The Boeing Company, Seattle, WA 98124, USA.
N. E. Pingitore Jr., Department of Geological Sciences, University of Texas at El Paso, El Paso, TX 79968–0555, USA.
F. W. Lytle, The EXAFS Co., Pioche, NV 89043, USA.

---

*To whom correspondence should be addressed. E-mail: nick@geo.utep.edu